

# *Lake surface water temperature [in "State of the Climate in 2021"]*

Article

Published Version

Carrea, L. ORCID: <https://orcid.org/0000-0002-3280-2767>, Merchant, C. J. ORCID: <https://orcid.org/0000-0003-4687-9850> and Woolway, R. I. ORCID: <https://orcid.org/0000-0003-0498-7968> (2022) Lake surface water temperature [in "State of the Climate in 2021"]. *Bulletin of the American Meteorological Society*, 103 (8). S28-S30. ISSN 1520-0477 doi: <https://doi.org/10.1175/2022BAMSStateoftheClimate.1>  
Available at <https://centaur.reading.ac.uk/107367/>

It is advisable to refer to the publisher's version if you intend to cite from the work. See [Guidance on citing](#).

To link to this article DOI:

<http://dx.doi.org/10.1175/2022BAMSStateoftheClimate.1>

Publisher: American Meteorological Society

All outputs in CentAUR are protected by Intellectual Property Rights law, including copyright law. Copyright and IPR is retained by the creators or other copyright holders. Terms and conditions for use of this material are defined in the [End User Agreement](#).

[www.reading.ac.uk/centaur](http://www.reading.ac.uk/centaur)

**CentAUR**

Central Archive at the University of Reading

Reading's research outputs online

The six datasets all agree that the last seven years (2015–21) were the seven warmest years on record. Similarly, the datasets agree that the global average surface temperature has increased at an average rate of  $0.08^{\circ}$ – $0.09^{\circ}\text{C decade}^{-1}$  since 1880 and at a rate more than twice as high since 1981 ( $0.18^{\circ}$ – $0.20^{\circ}\text{C decade}^{-1}$ , depending on the dataset).

The year began with a cold phase of the El Niño-Southern Oscillation (ENSO; see section 4b), also known as La Niña, across the eastern and central tropical Pacific Ocean, helping cool global temperatures slightly. The month of February had the smallest temperature anomaly of the year for the globe and was the coldest February since 2014, with global temperatures close to the 1991–2020 base period. La Niña dissipated by June, but re-emerged in August. With the exception of February, each month during 2021 had a global temperature that was above the 1991–2020 average.

While it is common, and arguably expected, for each newly completed year to rank as a top 10 warmest year (see Arguez et al. 2020), the global annual temperature for 2021 was considerably lower than we would expect due to the secular upward trend alone, with trend-adjusted anomalies registering between the 10th and 40th percentiles (depending on the dataset) following the Arguez et al. (2020) approach. These relatively cool conditions observed in 2021 are generally consistent with the typical cooling influence of La Niña. Moreover, trend-adjusted anomalies for 2021 are similar to the values recorded over the relatively cool years from 2011 to 2014, a period that also predominantly exhibited cooler-than-normal ENSO index values.

The year 2021 was characterized by above-average temperatures across much of the globe (Plate 2.1a; Appendix Figs. A2.1–A2.4), in particular across a large swath of North America (from the western United States to far northeastern Canada), as well as a region spanning northern Africa, western and central Asia, and into eastern Asia. Average to below-average temperatures prevailed across the central and eastern tropical Pacific Ocean and across parts of northwestern North America, Scandinavia, northern Russia, southern Africa, southern Australia, and parts of the southern oceans. Averaged as a whole, the global land-only surface air temperature for 2021 ranked among the sixth highest in the six datasets with a temperature departure of  $+0.32^{\circ}$  to  $+0.41^{\circ}\text{C}$ . The globally averaged SST was either sixth or seventh highest on record at  $+0.14^{\circ}$  to  $+0.22^{\circ}\text{C}$ , depending on the dataset.

Even though each dataset might differ slightly on the annual rankings and anomalies, it is worth noting that these differences are small and that, overall, temperature anomalies for each dataset are in close agreement (for more details see Simmons et al. 2017, 2021; Morice et al. 2021). Global atmospheric reanalyses use a weather prediction model to combine information from a range of satellite, radiosonde, aircraft, and other in situ observations to reconstruct historical weather and climate across the whole globe. While reanalyses may show regional differences from in situ surface temperature analyses because of regional model biases and changes in the observation network, they have been shown to agree well in well-observed regions (Simmons et al. 2017, 2021). Here, the data from ERA5 and JRA-55 are processed as described in Sanchez-Lugo et al. (2021).

## 2. LAKE SURFACE WATER TEMPERATURE—L. Carrea, C. J. Merchant, and R. I. Woolway

In 2021, the worldwide averaged satellite-derived lake surface water temperature (LSWT) warm-season anomaly was  $+0.60^{\circ}\text{C}$  with respect to the 1996–2016 baseline, the highest since the beginning of the record in 1995, comparable with 2016. The mean LSWT trend during 1995–2021 is  $+0.24^{\circ} \pm 0.01^{\circ}\text{C decade}^{-1}$  (Fig. 2.2a), broadly consistent with previous analyses (Woolway et al. 2017, 2018; Carrea et al. 2019, 2020, 2021). The warm-season anomalies for each lake are shown in Plate 2.1b, with 78% having positive (i.e., above-average temperature) and 22% negative (i.e., below-average) anomalies.

Globally, distinct regions of coherent above- and below-average LSWT anomaly can be seen. Almost half (45%) of the observed lakes show LSWT anomalies exceeding  $+0.5^{\circ}\text{C}$ , with 3% having anomalies higher than  $+3^{\circ}\text{C}$ . The highest positive anomalies were located across the Tibetan Plateau, in the northwest United States, and in the Middle East and Pakistan. Negative anomalies

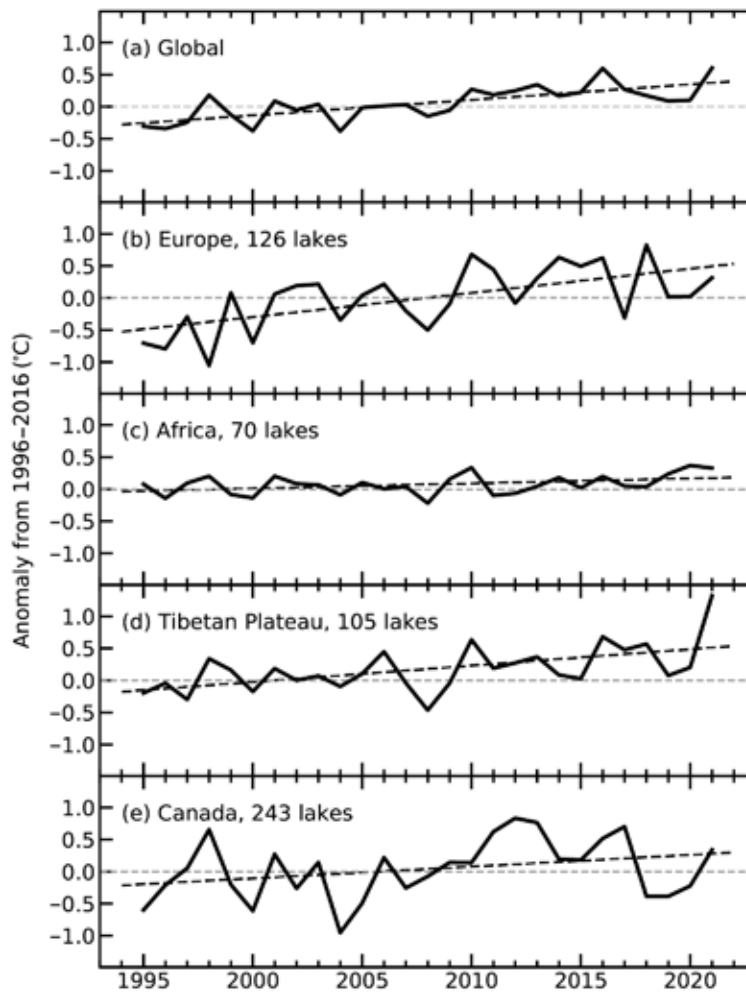


Fig. 2.2. Annual time series of satellite-derived warm-season lake surface water temperature anomalies (°C; 1996–2016 base period) from 1995 to 2021 for (a) more than 900 lakes distributed globally, (b) Europe, (c) Africa, (d) Tibet, and (e) Canada.

were mostly in South America (except Patagonia), Australia, and in high northern latitudes, including Alaska, Greenland, and eastern Russia (Plate 2.1b). Two lakes in the latter region had the most negative anomalies (below  $-3^{\circ}\text{C}$ ).

Four regions are considered in more detail: Canada, Europe, Tibet, and Africa (Fig. 2.3). The warm-season (July–September) LSWT anomalies calculated from the satellite data are consistent with the averaged surface air temperature (SAT) anomalies and show a warming tendency (from 1995) of  $+0.38^{\circ} \pm 0.03^{\circ}\text{C decade}^{-1}$  in Europe and  $+0.18^{\circ} \pm 0.03^{\circ}\text{C decade}^{-1}$  in Canada (Figs. 2.2b,e). In Africa, the tendency is closer to neutral ( $+0.08^{\circ} \pm 0.01^{\circ}\text{C decade}^{-1}$ ), while in Tibet the warming tendency has increased with respect to the previous years due to the exceptionally positive 2021 anomaly (Figs. 2.2c,d). In the Tibetan area, all but two lakes had positive anomalies in 2021, with an average of  $+1.3^{\circ}\text{C}$ . This is exceptionally high for the region, being 3.8 times the standard deviation of the average anomalies (1996–2016) and the highest on record. In Europe, below-average anomalies in northern Europe (29 lakes) are less prevalent than above-average anomalies (97 lakes), with an average anomaly of  $+0.31^{\circ}\text{C}$ . In Africa, 74% of the 70 lakes recorded positive anomalies. Several of the highest anomalies occurred north of the equator, contributing to an average continental anomaly of  $+0.33^{\circ}\text{C}$ . In Canada, 80% of the lakes had positive anomalies, with an average LSWT anomaly of  $+0.34^{\circ}\text{C}$ . The 2021 warm-season anomalies for Lakes Superior, Michigan, and Huron were computed using both in situ measurements and satellite data. The 2021 in situ anomalies were  $+3.36^{\circ}\text{C}$ ,  $+1.47^{\circ}\text{C}$ , and  $+1.00^{\circ}\text{C}$ , and the satellite were  $+2.49^{\circ}\text{C}$  (the highest on record),  $+0.85^{\circ}\text{C}$ , and  $+0.99^{\circ}\text{C}$ , respectively. The differences are mostly because the in situ measurements are taken at only some sites on the lake while the satellite observations

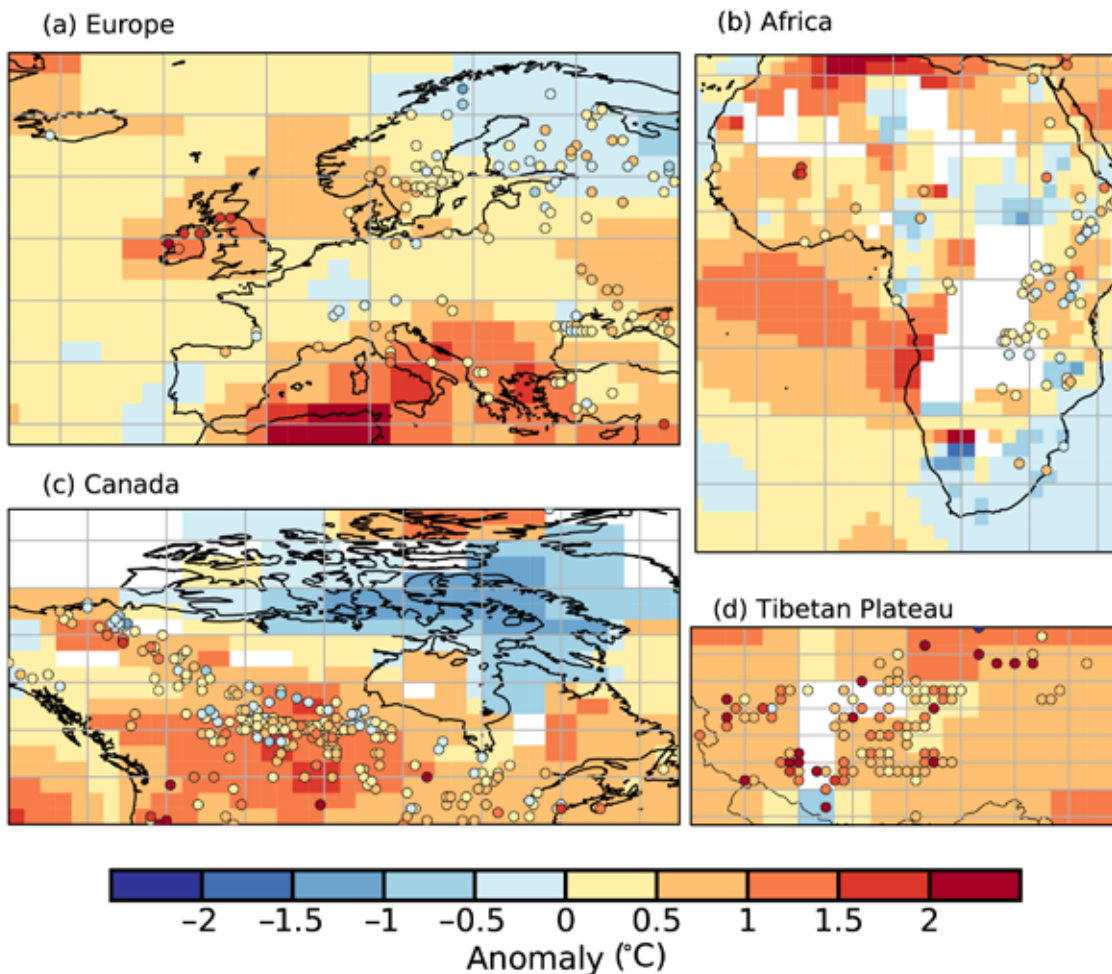


Fig. 2.3. Individual lake temperature anomalies (°C, colored dots) and 2-m air temperature anomalies (°C) in 2021 in (a) Europe, (b) Africa, (c) Canada, and (d) Tibet. These values were calculated for the warm season (Jul–Sep in the extratropical NH; Jan–Mar in the extratropical SH; Jan–Dec in the tropics) with reference to the 1996–2016 base period.

cover the whole lake. The spatial distribution of 2021 anomalies for these lakes (Appendix Fig. A2.5) all have positive values, but with strong variation across each of the lakes. The LSWT warm-season averages for midlatitude lakes are computed for summers, (July–September [JAS] in the extratropical Northern Hemisphere and January–March [JFM] in the extratropical Southern Hemisphere) and whole-year averages (January–December) are presented for tropical lakes (within 23.5° of the equator). LSWT time series were derived from satellite observations from the series of Along Track Scanning Radiometers (ATSRs), the Advanced Very High Resolution Radiometers (AVHRRs) on MetOp A and B (1996–2019), and the Sea and Land Surface Temperature Radiometers (SLSTRs) on Sentinel3A and 3B (2019–2021). The retrieval method of MacCallum and Merchant (2012) was applied on image pixels filled with water according to both the inland water dataset of Carrea et al. (2015) and a reflectance-based water detection scheme. The satellite-derived LSWT data are spatial averages for each of a total of 963 lakes, for which high quality temperature records were available in 2021. The satellite-derived LSWT data were validated with in situ measurements with a good agreement (average satellite minus in situ temperature difference less than 0.5°C). Lake-wide average surface temperatures have been shown to give a more representative picture of LSWT responses to climate change than single-point measurements (Woolway and Merchant 2018). The averaged surface air temperature was calculated from the GHCN v4 (250-km smoothing radius) data of the NASA GISS surface temperature analysis (Hansen et al. 2010; GISTEMP Team 2022). The in situ data for the Great Lakes were collected by the NOAA National Data Buoy Center.